Journal of Chromatography A, 1238 (2012) 1–10

Contents lists available at SciVerse ScienceDirect

Journal of Chromatography A

journal homepage: www.elsevier.com/locate/chroma

Review

Aqueous two-phase systems for protein separation: Phase separation and applications☆

Juan A. Asenjo, Barbara A. Andrews*

Centre for Biochemical Engineering and Biotechnology, Department of Chemical Engineering and Biotechnology, Institute for Cell Dynamics and Biotechnology: A Centre for Systems Biology, University of Chile, Santiago, Chile

ARTICLE INFO

Article history:
Received 31 January 2012
Received in revised form 13 March 2012
Accepted 15 March 2012
Available online 23 March 2012

Keywords:
Aqueous two-phase systems
Phase separation
Applications

ABSTRACT

Aqueous two-phase systems (ATPS) that are formed by mixing a polymer (usually polyethylene glycol, PEG) and a salt (e.g. phosphate, sulphate or citrate) or two polymers, and water can be effectively used for the separation and purification of proteins. The partitioning between both phases is dependent on the surface properties of the proteins and on the composition of the two phase system as has been recently reviewed by Asenjo and Andrews [1]. This paper analyses and reviews some elements that are important for implementation of these processes which are related to phase separation and continuous processing of ATPS. Phase separation for ATPS formed by PEG and salts has been studied and has been found to depend on which of the phases is continuous. Profiles of dispersion heights can be represented as a fraction of the initial height and are independent of the dimensions of the separator. This is important for the design of large scale aqueous two-phase separations. The kinetics of phase separation has been investigated as a function of the physical properties of the system. The settling rate is a crucial parameter for equipment design and it has been studied as a function of viscosity and density of the phases as well as the interfacial tension between them. Correlations that describe the rate of phase separation have been developed. Working in a continuous bottom-phase region is advantageous to ensure fast separation. A mathematical model to describe the continuous, study state operation of these systems has been investigated. Two simulations to show the effect of phase ratio on purification have been carried out which clearly show the effectivity of using such models. The practical application of ATPS has been demonstrated in many cases including a number of industrial applications with excellent levels of purity and yield. Examples include the purification of α-amylase and the large scale "in situ" purification of IGF-1 carried out by Genentech. The production scale purification of chymosin from recombinant Aspergillus supernatant is the most successful industrial application of this technology. Other applications include the separation and purification of human α-antitrypsin from transgenic sheep milk, the purification of monoclonal antibodies, tPA from CHO supernatant and recombinant VLPs (virus like particles) from yeast cells.

Contents

☆ Presented at the 16th International Conference on BioPartitioning and Purification, Puerto Vallarta, Jalisco, Mexico, 18–22 September 2011.

* Corresponding author. Tel.: +56 2 9784710; fax: +56 2 6991084.
E-mail address: bandrews@ing.uchile.cl (B.A. Andrews).

0021-9673/$ – see front matter © 2012 Elsevier B.V. All rights reserved.
doi:10.1016/j.chroma.2012.03.049

1. Introduction

Two phase aqueous partitioning is a very mild method of protein purification, and denaturation or loss of biological activity are not usually seen. This is probably due to the high water content and low interfacial tension of the systems which will protect the proteins. The polymers themselves may also have a stabilizing effect. Aqueous two-phase partitioning can be used to separate proteins from cell debris or to purify proteins from other proteins. Most soluble and particulate matter will partition to the lower, more polar phase, whilst proteins will partition to the top, less polar and more hydrophobic phase, usually PEG [1–4]. Separation of proteins from one another is achieved by manipulating the partition coefficient by altering the average molecular weight of the polymers, the type of ions in the system, the ionic strength of the salt phase, by adding an additional salt such as NaCl or the presence of hydrophobic groups [5–7].

The partition coefficient (K) is defined as

$$K = \frac{C_T}{C_B} \quad (1)$$

where C_T and C_B represent the equilibrium concentrations of the partitioned protein in the top and bottom phases, respectively.

The following properties of partitioning can be exploited individually or in conjunction to achieve an effective separation of a particular protein [1].

(i) Hydrophobicity, where the hydrophobic properties of a phase system are used for separation according to the hydrophobicity of proteins.
(ii) Electrochemical, where the electrical potential between the phases is used to separate molecules or particles according to their charge.
(iii) Size-dependent partitioning where molecular size of the proteins or surface area of the molecules (proteins) or particles is the dominating factor.
(iv) Biospecific affinity, where the affinity between sites on the proteins and ligands attached to one of the phase polymers is exploited for separation.
(v) Conformation-dependent, where the conformation of the proteins is the determining factor.

Thus, the overall partition coefficient can be expressed in terms of all these individual factors:

$$K = K_0 \cdot K_{hfob} \cdot K_{el} \cdot K_{biosp} \cdot K_{size} \cdot K_{conf} \quad (2)$$

where hfob, el, biosp, size and conf stand for hydrophobic, electrochemical, biospecific, size and conformational contributions to the partition coefficient and K_0 includes other factors.

The factors which influence partitioning of a protein in aqueous two-phase systems are:

(i) molecular weights/size of polymers;
(ii) concentration of polymer;
(iii) ionic strength of the salt;
(iv) pH;
(v) additional salt used such as NaCl that increases the hydrophobic resolution of the system.

Generally, the higher the molecular weight of the polymers the lower the concentration needed for the formation of two phases, and the larger the difference in molecular weights between the polymers the more asymmetrical is the curve of the phase diagram [3].

During the last few years there has been renewed interest in separation methods for biological molecules as alternatives to chromatography. Chromatography involves high costs, batch operation, low throughput and complex scale-up [8]. Aqueous two-phase systems have recently been proposed for antibody purification [9–11]. Rosa et al. [10] studied the economic and environmental sustainability of an ATPS process compared to protein A chromatography. The ATPS process was found to be advantageous in terms of process economics when processing high titer cell supernatants.

2. Phase formation and kinetics and phase separation

Why do systems with a continuous top phase take longer to separate than systems with a continuous bottom phase? It appears that the balance of forces on the drops during coalescence is different in each case. In general, three forces are acting on a drop during coalescence: gravitational, flotation and frictional, as shown in Fig. 1 [12]. The movement of a drop depends on the balance between these forces. The gravitational force depends on the density of the drops, flotation or frictional forces depend on the rheological properties of the phases. The frictional force always impedes drop movement. These forces together with the interfacial tension, determine the coalescence behaviour and the characteristics of the dispersed phase. In ATPS the densities of phases are very similar so it is the flotation forces which determine the behaviour of the drops. The ratio of the viscosities of the polymer and the salt phase can be very large (5–50 times), the salt phase being much less viscous than the polymer phase. When the bottom phase is discontinuous, the coalescing drops must descend through the polymer phase. As the polymer phase has a higher viscosity, the friction between the drops and the phase is high, hence the separation time is longer. When the bottom phase is continuous drops of the top phase move through the bottom phase, which has a much lower viscosity, favouring coalescence.

An important element is which phase will be continuous and which the dispersed. Settling rates have been studied in PEG/salt ATPS [12,13]. Given the high viscosity, rates are much smaller when the PEG top phase is the continuous phase. Phase separation times for polyethylene glycol (PEG)-4000-phosphate aqueous two-phase systems have been studied [14], for small scale (5-g) and larger scale (1300-g) systems. Profiles of dispersion height for both larger and small scale systems were represented as a fraction of the initial height and were found to be independent of the geometrical dimensions of the separator. Furthermore, by plotting time as a fraction of the initial height the total time of separation can be calculated for a given height of system in a particular system as shown in Fig. 2a for systems of two different sizes. This generalization is important for the design of large scale aqueous two-phase separators. Phase separation times were also found to be dependent on which of the phases is continuous. A characteristic change in phase separation time was also observed at the phase inversion point (i.e. where the dispersed phase changes to a continuous phase and vice versa) and

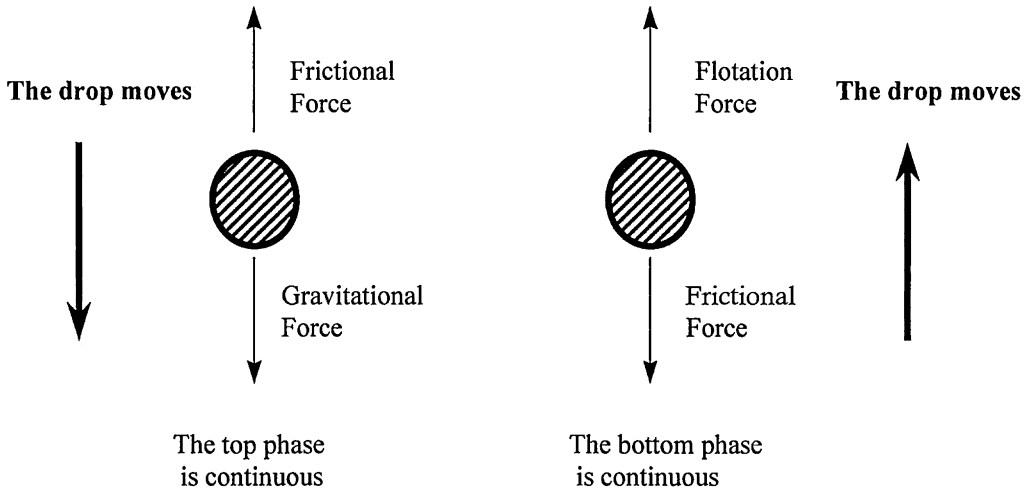

Fig. 1. Diagram showing the different forces acting on a drop depending on which phase is continuous [12].

this point tends toward higher volume ratios as the tie-line length (TLL) is increased. Furthermore, the phase inversion point at each TLL corresponds to a fixed phosphate concentration for this system as shown in Fig. 2b.

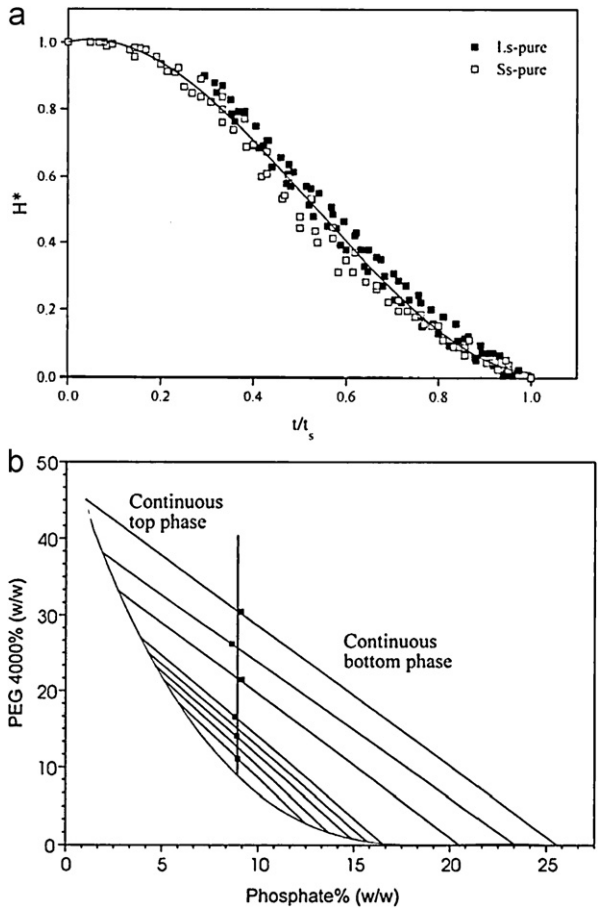

Fig. 2. (a) Change in the relative separation time (t/t_s) with relative height of dispersion ($H^* = H/H_0$) for 5-g (Ss = small scale; open symbols) and 1300-g (Ls = large scale; closed symbols) systems. Third order polynomial fit with $R = 0.95$ [13]. (b) Phase diagram PEG-4000-phosphate at pH 7, phase inversion point (■). To the left of the vertical line, systems have a continuous top phase and to the right a continuous bottom phase [13].

For the determination of the TLs, a simple gravimetric method can be used [15] which makes unnecessary any chemical analysis [1].

3. Phase separation and kinetics

The separation of the equilibrated phases after their formation is a time-dependent process [13]. A typical batch separation profile is shown in Fig. 3. From the figure, it can be seen that until the system is fully settled three regions exist, the top phase, the bottom phase and the dispersion. When the top phase is continuous, drops of dense bottom phase exist in the top phase, and these sink so that the top most drops form a settling front, this indicates that the process of coalescence is slower than droplet descent. The drops accumulate and coalesce at the boundary of the dispersion region and the bottom phase forming a coalescing front. From Fig. 3, it can be seen that at time t, the height of the dispersion is given by h_t and is calculated as the distance between the settling front and the coalescing front at time t. During batch separation, the initial system is entirely mixed, resulting in one large dispersion region and hence a large h. With time, the phases separate and h_t decreases in size until the systems is entirely separated.

Kaul et al. [14], identified the continuous phase by visual observation using two pairs of PEG-4000-phosphate systems, each pair

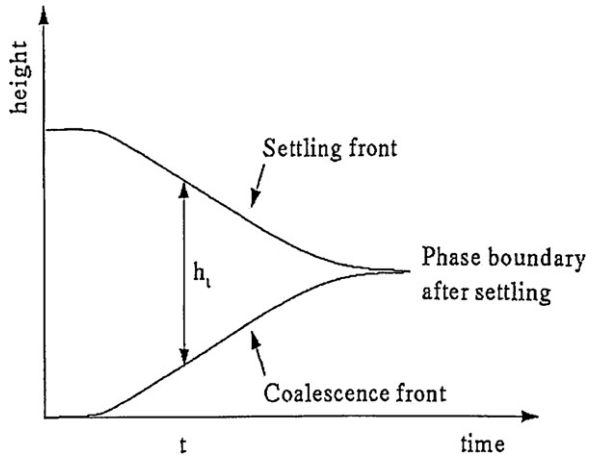

Fig. 3. Batch separation profile when the bottom phase is dispersed. The height of the dispersion decreases from the initial value (total height) to zero as clear top and bottom phase [13].

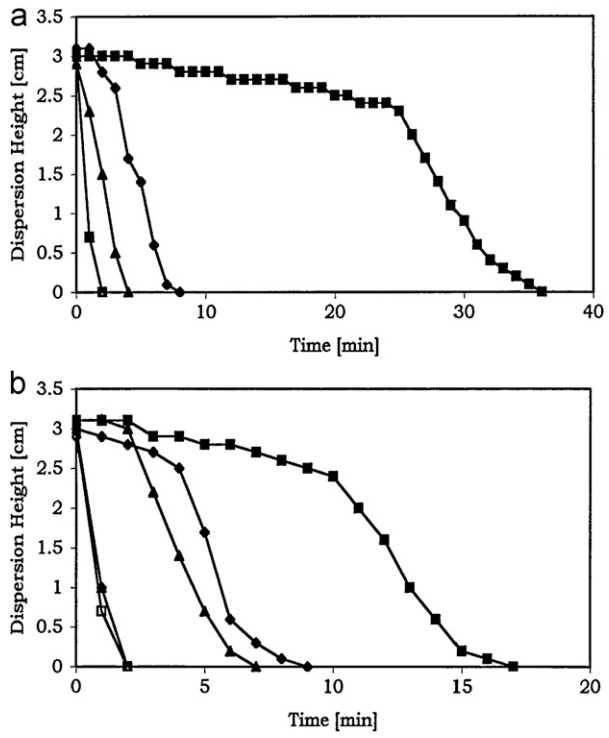

Fig. 4. Dispersion height vs. time for PEG 1500/sulphate systems with different mass ratios (R) with extract of *B. subtilis*. The full (dark) symbols are systems with a continuous top phase, the open (empty) symbols are systems with a continuous bottom phase; (a) (■) $R = 9$, (♦) $R = 5.2$, (▲) $R = 3.14$, (□) $R = 13$, (◊) $R = 1$, (△) $R = 0.7$, (b) (■) $R = 5$, (♦) $R = 4.16$, (▲) $R = 2.75$, (□) $R = 1.72$, (◊) $R = 1.23$ and (△) $R = 0.875$ [12].

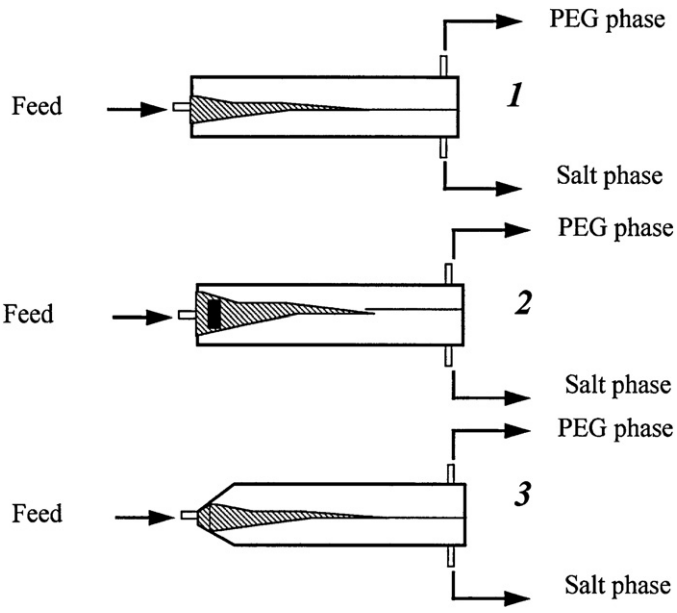

Fig. 5. Settler inlet geometries: (1) square; (2) square with bafle; (3) prismatic [12].

were on the same tie-line but had different volume ratios. One tie-line was relatively near the binodial curve (phosphate 10.7%, w/w, PEG-4000 12.5%, w/w) and the other (phosphate 21.93%, w/w, PEG-4000 25.62%, w/w) was on a tie-line far from the binodial curve. The observations confirmed that the rate of sedimentation is high and the rate of coalescence controls the kinetics of phase separation [14]. Phase separation is much more rapid when the bottom phase is continuous since the viscosity of this phase is much smaller.

Salamanca et al. [12], studied the kinetics of phase separation in PEG/salt systems. In PEG 1500/sulphate systems with different volume ratios at two distances from the binodial curve it was found that as the volume ratio (R) decreases, the phase separation time is shorter and, that at the larger volume ratios there is an apparent "lag" time during which there is almost no decrease in the dispersion height. Fig. 4 shows phase separation in PEG 1500/sulphate systems in the presence of extract of *Bacillus subtilis*. As in the systems without extract, systems with a continuous bottom phase separate more quickly than those with a continuous top phase. It is evident that the presence of cell extract has an important effect on phase separation time. All systems with a continuous top phase take longer to separate in the presence of *Bacillus* supernatant. This difference in separation time can be due to a number of factors caused by the material added (*Bacillus* supernatant) which include properties of the proteins and other molecules added and their interaction with the phase system which will affect the charge and size of the drops and the hydrophobicity, and thus their surface properties.

Salamanca et al. [12], did continuous studies in a settler with three inlet geometries (Fig. 5). The dispersion height was measured as a function of separator length at different injection velocities, which resulted in different linear velocities in the settler, in the presence and absence of extract of *B. subtilis* [12]. In the absence of *B. subtilis* extract there is very little difference between all three geometries. The presence of extract makes little difference which would be expected in systems where the bottom phase is continuous. In this case however, the higher linear velocities give slightly shorter separation lengths along the settler for the square inlet configuration with baffle. The geometry of the square inlet with a baffle also prevents the accumulation of dispersion in the corners of the settler and stops the formation of "macrofluids" which hinder the adequate flow of dispersion into the settler [12].

4. Phase separation rates: correlation with system properties

As has been stated before the question of which phase is the continuous one in an ATPS is extremely important and has been addressed [13–15]. It has been shown that there is a point of transition where continuity switches from one phase to the other (phase inversion point). A locus of phase inversion points was found, creating a phase inversion line (or rather, a phase inversion band) that delimited on the phase diagram between a region where the top phase is continuous and a region where the bottom phase is continuous. To investigate this transition, six points on either side of the phase inversion line were chosen and are shown in Fig. 6a [13]. The figure shows the phosphate/PEG concentration plane. In Fig. 6a, the tie lines are parallel; hence tie line length (TLL) is proportional to the difference in PEG concentration between top and bottom phases. The points shown in Fig. 6a correspond to 14, 16, 18, 20, 22, and 24% PEG 4000 at 8 and 10% phosphate. The viscosity, density, interfacial tension, and rate of phase separation were measured for each of these 12 systems.

4.1. Effect of tie line length on the viscosity, density and interfacial tension between the phases

The viscosities of both top and bottom phases for all the points shown in Fig. 6a can be seen in Fig. 6b. The longer the TLL, the higher the concentrations of PEG in the top phase and therefore the higher the viscosity in the top phase. On the other hand, with longer TLL, the decrease in PEG concentration in the bottom phase is very small whereas the increase in salt concentration is large (Fig. 6b). This has hardly any effect on the viscosity of the bottom phase. Hence, the viscosity of the top phase and the viscosity difference increase as the TLL increases. At the lowest TLL, it is ten times larger than the

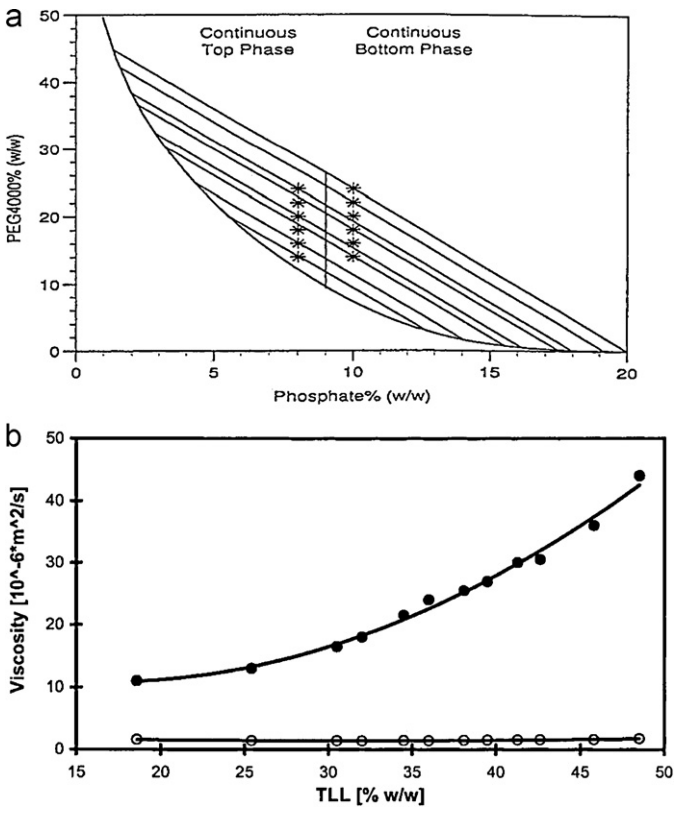

Fig. 6. (a) Experimental systems studied with some of the associated tie lines [13]. (b) Viscosity of the top phase and the bottom phase as a function of TLL. (●) top phase and (○) bottom phase [13].

viscosity of the bottom phase, but at the largest TLL it becomes more than forty times larger.

The density of the top and bottom phases as a function of the TLL was also measured [13]. In contrast to the effect of TLL on viscosity, the variation in density of the top phase is very small and practically negligible when compared to the strong influence of TLL on the density of the bottom phase. This is due to the fact that, as the TLL becomes longer, the phases become closer to solutions of pure PEG in the top, and pure phosphate in the bottom. PEG concentration has a small influence on density, whereas phosphate concentration affects the density much more strongly.

The effect of TLL on the interfacial tension can be seen in Fig. 7. The interfacial tension is seen to increase over the range studied and varies over two orders of magnitude in the region of interest. As TLL

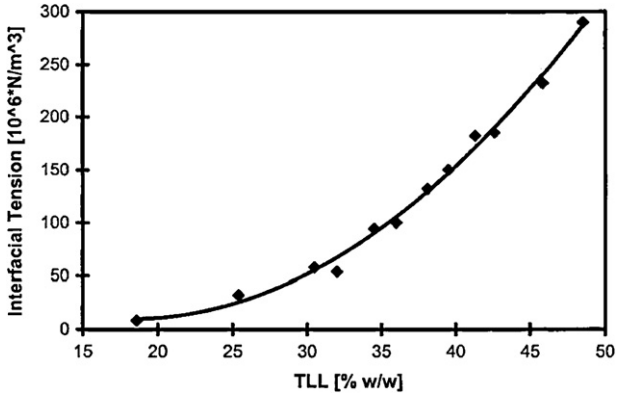

Fig. 7. Variation in the interfacial tension between the phases as a function of TLL [13].

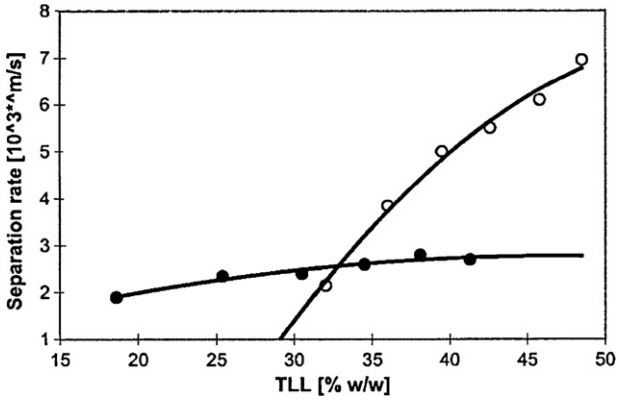

Fig. 8. Rates of phase separation measured in the top-phase continuous and bottom-phase continuous systems, as a function of TLL. (●) top phase continuous and (○) bottom phase continuous. The solid line represents the fitting of Eqs. (3) and (4) to the data points measured in the top phase continuous and bottom phase continuous regions [13].

increases, the difference between the top and bottom phase composition becomes greater and hence the interfacial tension increases.

4.2. Rate of separation; rate data correlation

A dimensionless correlation that takes into account the effects of viscosity, particularly of the continuous phase, density difference between the phases and interfacial tension was investigated with respect to an aqueous two phase system [13]. This equation was fitted to the experimental values found in order to calculate the values of the constants. For the continuous top phase the dimensionless equation found was:

$$\left(\frac{dh}{dt}\right)\left(\frac{\mu_C}{\sigma}\right) = 1.435\times10^{-5}\left(\frac{\mu_C}{\mu_D}\right)^{2.148}\left(\frac{\Delta\rho}{\rho_C}\right)^{-1.062}\left(\frac{\sigma}{\sigma_w}\right)^{-0.971} \quad (3)$$

where μ_C is the viscosity of the continuous phase, μ_D is the viscosity of the dispersed phase, ρ_C is the density of the continuous phase, σ is the interfacial tension between the two phases, σ_w is the surface tension of the air–water interface at 20 °C (7.28×10^{-2} N m^{-1}).

Eq. (3) shows that the rate of separation in the top continuous-phase region is dependent on the viscosity and density difference. The equation was fitted to the experimental data points and can be seen in Fig. 8 (represented by the solid line) to give a very good fit to the experimental values.

Using the values found for the bottom continuous-phase region, the dimensionless equation found was:

$$\left(\frac{dh}{dt}\right)\left(\frac{\mu_C}{\sigma}\right) = 2.04\times10^{-5}\left(\frac{\mu_C}{\mu_D}\right)^{0.144}\left(\frac{\Delta\rho}{\rho_C}\right)^{-0.555}\left(\frac{\sigma}{\sigma_w}\right)^{-0.079} \quad (4)$$

Viscosity is far less important in the bottom phase continuous region and thus the dependence of the rate of phase separation (dh/dt) is much weaker than in Eq. (3). Density difference does play a role but less strongly than in Eq. (3). A very good fit Eq. (4) to the experimental points was found as shown in Fig. 8 (represented by the solid line).

The values of the constants found show the differences between the two regions. The viscosity of the continuous phase is the most important factor affecting the rate of separation in the continuous top phase region. This is followed by the density difference. In the continuous bottom phase, the density ratio is almost-twice as dominant as the viscosity ratio and the interfacial tension.

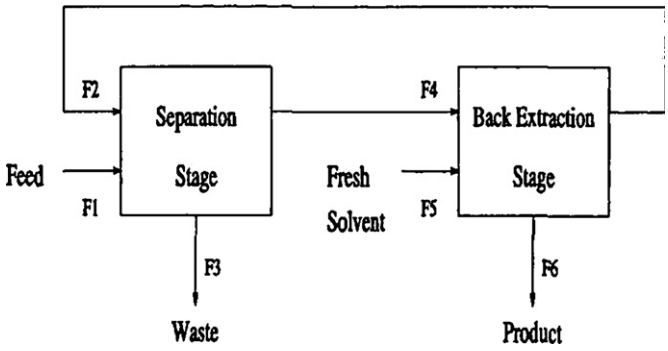

Fig. 9. Flow scheme of process [16].

When the bottom phase is continuous the effect of density, viscosity and interfacial tension result in a 3.5-fold change in the separation rate (Fig. 8) over the range studied. When the top phase is continuous all three factors play a much less important role. Density is the most important of the three. Over the range studied the settling rate only changes by 50%.

5. A mathematical model of aqueous two-phase continuous protein extraction

5.1. Model of protein separation

Fig. 9 shows the flow scheme of the process used in a model used for the simulation of ATP continuous extraction [16]. The first stage is the major separation step. Target and contaminant proteins enter the process (separation stage) via stream F1, either in the form of whole or disrupted cells or just soluble proteins after cell debris removal. The recycle stream F2 from Stage 2 (back extraction stage) consists of the top PEG phase after back extraction of the product protein into the salt phase. A high NaCl concentration aids protein partitioning to the top phase in Stage 1 whilst the partitioning of the contaminants is unaffected and leaves via the bottom phase waste stream, F3, with virtually no product. Stream F4 passes on the product rich top phase to Stage 2 for back extraction. Fresh PEG and phosphate are continuously added in Stage 1 to account for phase component losses from the system. Extra phosphate is added by stream F5, to dilute the NaCl concentration. This aids product partitioning back into the lower phosphate phase. The top phase is then recycled to minimize PEG loss and also increase the process yield. F6 is the final product output stream from the bottom phase of Stage 2. The mathematical model of the process was composed of mass balances and phase equilibrium relationships as described below.

5.2. Mass balances

The steady state mass balances account for the main component, i.e. flow-rates, phase forming chemicals and the proteins present in both stages.

$$\sum_{\text{in}} F_i = \sum_{\text{out}} F_i \tag{5}$$

$$\sum_{\text{in}} F_i P_i = \sum_{\text{out}} F_i P_i \tag{6}$$

$$\sum_{\text{in}} F_i X_i = \sum_{\text{out}} F_i X_i \tag{7}$$

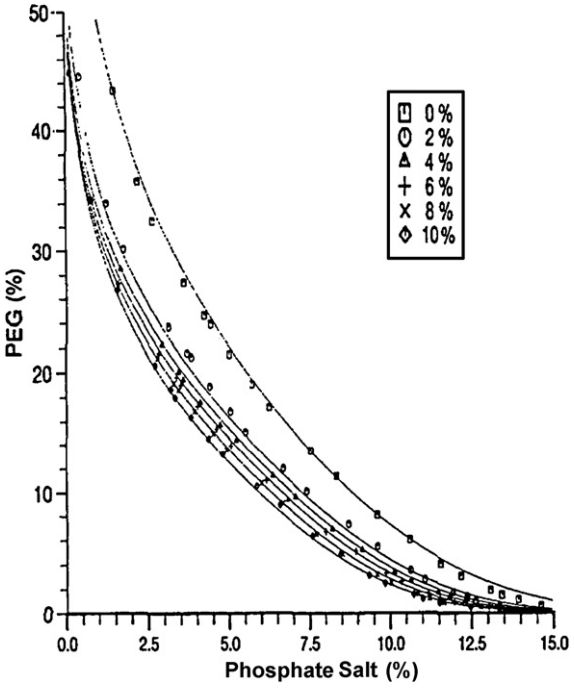

Fig. 10. Close-up of experimental points and fitted lines for the binodials at different NaCl concentrations [16].

where i is the stream number, F is the flow-rate ($m^3\,s^{-1}$), P is the phosphate, PEG or NaCl concentration ($kg\,m^{-3}$) and X is the product or contaminant concentration ($kg\,m^{-3}$).

These equations are written for each stage j.

5.3. Phase equilibrium

The phase equilibrium for an aqueous two-phase system can be represented as a binodial curve relating the phosphate and PEG concentrations. The binodial is known to vary in the presence of NaCl, so this was modelled over the range of 0–10% NaCl. The binodial data for a PEG 4000-phosphate system at pH 7 was collected and fitted to an equation of the form:

$$\ln(Y) = A + BX^3 + C\sqrt{X} \tag{8}$$

where Y is the PEG concentration and X is the phosphate concentration.

The constants A, B and C are functions of the NaCl concentration.

A function relating the partition coefficient to the concentration of NaCl was fitted. The partition behaviour of α-amylase [17] was studied to show the effect of the salt concentration on the partition coefficient (K_p). The partition behaviour of the protein as a function of NaCl concentration in the system was fitted to a sigmoidal Boltzmann curve of the form:

$$\log K_p = \frac{G_1}{1 + \exp\{(\text{NaCl} - G_3)/G_4\}} + G_2 \tag{9}$$

Partitioning of contaminants was much simpler and could be modelled by a straight line as they were not a strong function of the concentration of NaCl.

$$\log K_C = E_1 \text{NaCl} + E_2 \tag{10}$$

where G and E are constants.

5.4. Binodial and partition coefficient fitting

Fig. 10 shows the fitting of the binodial curves with the experimental points. It can be seen that the empirical equation used gave

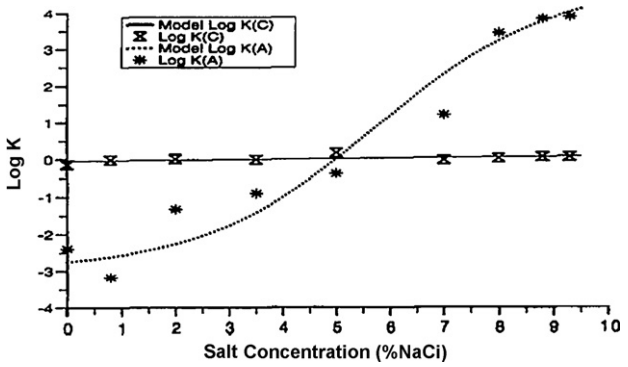

Fig. 11. Comparison of α-amylase (A) and contaminants (C) data and model fit [16].

an excellent fit to the data and was used to model the binodial over the continuous range of NaCl concentrations from 0 to 10%.

The sigmoidal Boltzmann equation used to express the α-amylase data grave a very good fit to the experimental values as illustrated in Fig. 11. Some of the discrepancy seen at the very low values of log K_p can be attributed to the error associated with the measurement of very low protein concentrations ($K = 10^{-2}$–10^{-3}). Protein contaminants were fitted by a straight line (Eq. (10)).

5.5. Simulation examples: small PEG phase or large PEG phase

The complete model has been successfully used to study two very different cases. [16]. The first consisted of running the model with a large bottom phase and a small top phase in both stages. Since the contaminants have a K value ca. 1.0 ($\log K = 0$) this allows the separation of a large fraction into the first bottom phase and their elimination in F3 (Fig. 9). It also allows the NaCl to be significantly diluted when the PEG is transferred into the second stage. A large fresh phosphate phase (F5) is added as shown in Fig. 9 thus obtaining dramatically different partition coefficients for the product protein in Stage 1 (K1) and Stage 2 (K3) as shown in Figs. 11 and 12. The overall system diagram of material balances is shown in Fig. 13. M1 and M2 represent the overall composition of Stages 1 and 2 which are theoretical "operating points" of both stages and represent large bottom phases and small top phases. The two binodials shown correspond to the NaCl concentrations of the stages, 8.8% and 2.0% respectively. The "lower" binodial (towards the left) is the one with 8.8% NaCl (Stage 1, separation). The numbers 1, 3, 2, etc. represent the fluxes F1, F3, F2, etc. in the process diagram in Fig. 9. Such a system diagram of material balances is a very clear representation of an extraction and back-extraction system. A large purification factor is obtained for the protein product (α-amylase) in this system. As shown by Mistry et al. [16], running

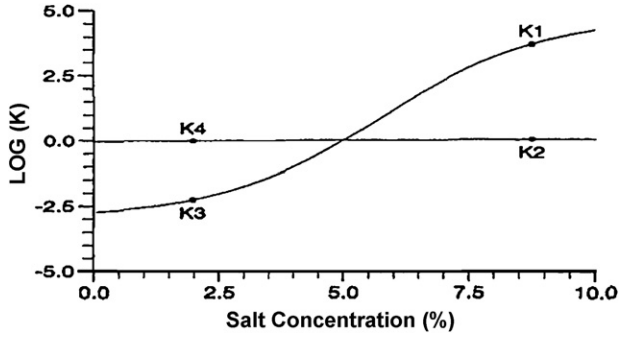

Fig. 12. Partition coefficients for system with small PEG and large phosphate phases thus allowing for important NaCl dilution between Stage 1 (K1, K2) and Stage 2 (K3, K4) [16].

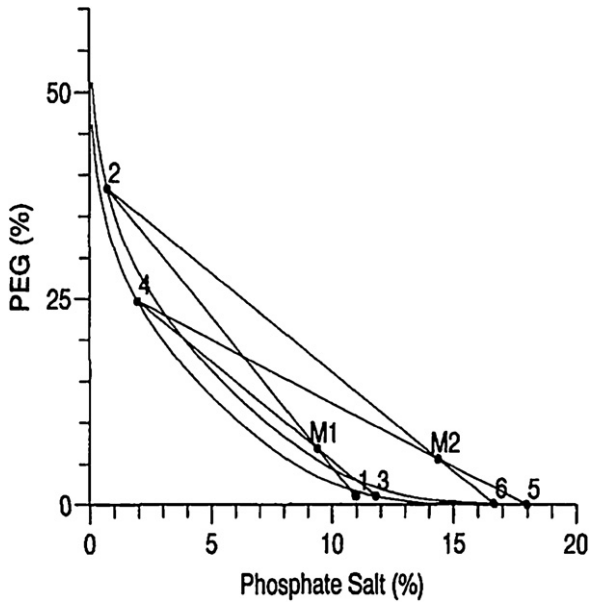

Fig. 13. Overall system diagram for systems with large bottom phases. M1 and M2 represent overall composition of Stages 1 and 2. Numbers refer to streams (F1, F2, etc.). The two binodials correspond to NaCl concentrations of 8.8% and 2.0% respectively [16].

the model with large top phases in both stages only gives a relatively small dilution of the NaCl between stages (e.g. 5.9% and 4.3% respectively) thus resulting in a much smaller change in the partition coefficients between Stages 1 and 2 (K1 and K3). The large top phase in the separation stage (see Figs. 9 and 11) also resulted in a larger amount of contaminant proteins giving a much smaller purification factor.

6. Applications

Extensive research concerning the application of ATPS for the recovery and partial purification of therapeutic and other proteins of industrial interest has been conducted [1,18,19]. For expensive proteins for medical applications, multistep chromatography, which usually includes ion-exchange, hydrophobic interaction and in many cases affinity chromatography, which are operated in a batch mode, has proven to be reliable and hence the method of choice. However with the trend of larger scale processes and more competitive production worldwide the possibility of using continuous processes, that can be readily scaled up, such as ATPS, becomes evidently more attractive. Table 1 shows some of the proteins that have been readily separated in such systems.

It was found that when adding important concentrations of NaCl (up to 10%) to PEG/salt systems the partition coefficient of the protein thaumatin, could be directed to the more hydrophobic PEG phase [20]. Later, it was shown that this effect could be much more dramatically observed for the very hydrophobic protein α-amylase. [17]. Fig. 14 shows the dramatic change in the partition coefficient

Table 1
Proteins which have been successfully purified using ATPS.

- Thaumatin
- α-Amylase
- IGF-1 (in situ extraction from *E. coli*)
- Monoclonal antibodies, IgG
- Transgenic AAT (human α-antitrypsin) from sheep milk
- Chymosin
- tPA (tissue plasminogen activator) from CHO supernatant
- Recombinant VLPs (virus like particles) produced in yeast

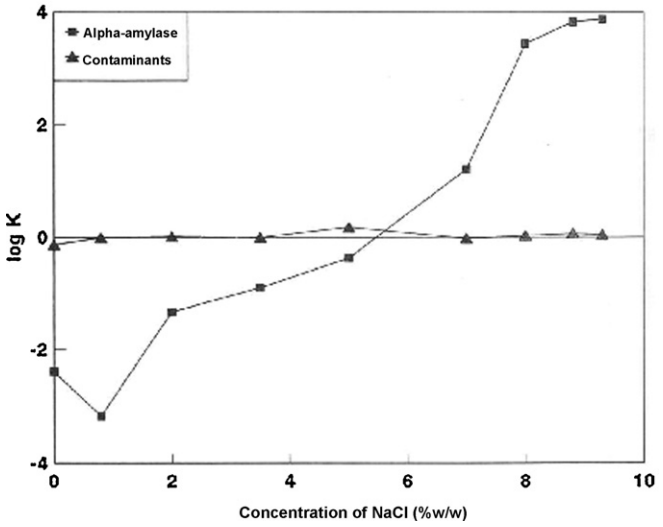

Fig. 14. Partition behaviour of α-amylase ($\log K_a$) and contaminant protein ($\log K_c$) from industrial supernatant from *B. subtilis* fermentation in PEG 4000/sulphate systems as a function of added NaCl concentration at pH 7 and phase volume ratio of 1 [17].

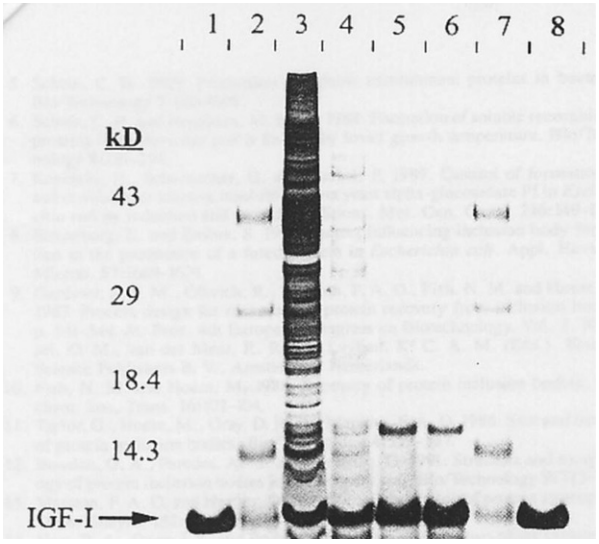

Fig. 15. Silver stained, reduced SDS–PAGE gel illustrating purification of non-native IGF-I during isolation by in situ solubilization and aqueous two-phase extraction. The different lines contain the following: (1) purified IGF-I standard; (2) molecular weight standards; (3) fermentation broth; (4) in situ solubilization supernatant; (5) isolated light phase; (6) isolated pellet from pH 7 precipitation; (7) molecular weight markers; and (8) purified IGF-I standard. The position of IGF-I is indicated by the arrow [21].

of α-amylase in a PEG 4000/sulphate system when adding 8% NaCl. In this case, as has already been discussed, a high NaCl would be used for the protein extraction and a low NaCl concentration for the back extraction.

Hart et al. [21] investigated the separation and purification of Insulin like Growth Factor (IGF-1) in a PEG 8000/salt ATPS formed with the actual fermentation broth and *Escherichia coli* cells. Thus this constitutes an in situ isolation of the protein from the "permeabilised" *E. coli*. After the fermentation stage of intracellular IGF-1, the cells were permeabilised using a strong denaturing agent such as urea. This produced the permeabilisation of the *E. coli* walls and extraction of denatured IGF-1 into the supernatant. PEG 8000 was then added to generate an ATPS in which the denatured protein partitioned almost exclusively to the more hydrophobic top phase. Fig. 15 shows the levels of recombinant protein in the supernatant of the fermentation before extraction (lane 3) and after extraction (lane 4) where it is possible to observe that virtually all the intracellular recombinant protein has been extracted and that contaminant proteins represent a very small amount *vis-à-vis* the recombinant IGF-1. A 70% cumulative recovery with 97% product purity of the denatured, and thus very hydrophobic, protein was obtained and the process was scaled-up up to 1000 l.

A similar effect to that shown by α-amylase was observed very interestingly, for the partition and purification of monoclonal antibodies which are also very hydrophobic proteins [22]. An industrial serum free, crude, concentrated culture supernatant of hybridoma produced murine IgG, with a relatively low level of protein contaminants (14% IgG purity) was processed in this system. After the back extraction the contaminants were reduced 18 fold giving IgG with 80% purity. A 5.9 fold purification was obtained out of a 7.3 maximum possible (at 100% pure IgG) [22]. Fig. 16 shows the level of contaminants and monoclonal antibodies in the first separation and in the back extraction. The peak on the right shows the level of antibody in the top phase (a) and in the bottom phase (b) in the first extraction. Clearly virtually all the monoclonals are in the top phase in the first extraction. In the second "back-extraction" the monoclonals partition into the bottom phase (d). All of the IgG was recovered. This pioneering finding was later exploited in detail investigating the partitioning and important scale up and processing factors of the very hydrophobic MAbs in ATPs [23].

Guan et al. [24] reported the use of a two-stage ATPS extraction strategy for the recovery and purification of human recombinant interferon α1 (rhIFN-α1) expressed in genetically modified *E. coli*. Transgenic sheep milk containing the protein human α-antitrypsin (AAT) was partitioned in (PEG)-sulphate and PEG-phosphate biphasic systems. [25] Individual partition coefficients for AAT and some of the milk proteins were determined in these systems. The effects of PEG molecular weight, pH and the inclusion of NaCl on the partitioning of the proteins were also studied. It was found that increasing the concentration of NaCl and decreasing the molecular weight of the PEG resulted in an increase of the partition coefficients of the proteins to the upper (PEG) phase. This partitioning effect was greater for the more hydrophobic proteins and particularly in systems having a pH close to the isoelectric point of the protein. Under the most favourable conditions using a 4% (w/w) loading of transgenic ovine milk, a 91% yield of AAT in the PEG phase with a purity of 73% was obtained.

The separation and purification of recombinant calf chymosin expressed in the fungus *Aspergillus awamori* [26] was probably the first recombinant protein to be separated commercially and at a large scale using ATPS. Some details of this separation are shown in Table 2.

Another very hydrophobic protein that has been separated using such systems is tPA (tissue plasminogen activator). Details of this separation are shown in Table 3 [27,28].

Table 2
Application of two phase liquid–liquid extraction to the purification of calf chymosin from *A. awamori* (Hayenga et al. [26]).

- Chymosin from bovine calf in filamentous fungi *A. awamori*
- Glycoamylase-prochymosin fusion protein
- Majority found in the culture medium as mature chymosin
- The fungus also secretes other enzymes that may have detrimental effects in either cheese making or whey by products
- Current industrial enzyme purification techniques not cost effective
- We designed recovery process two phase liquid-liquid extraction PEG 8000/Na_2SO_4
- Meets the purity and cost objectives
- Partition coefficients greater than 100

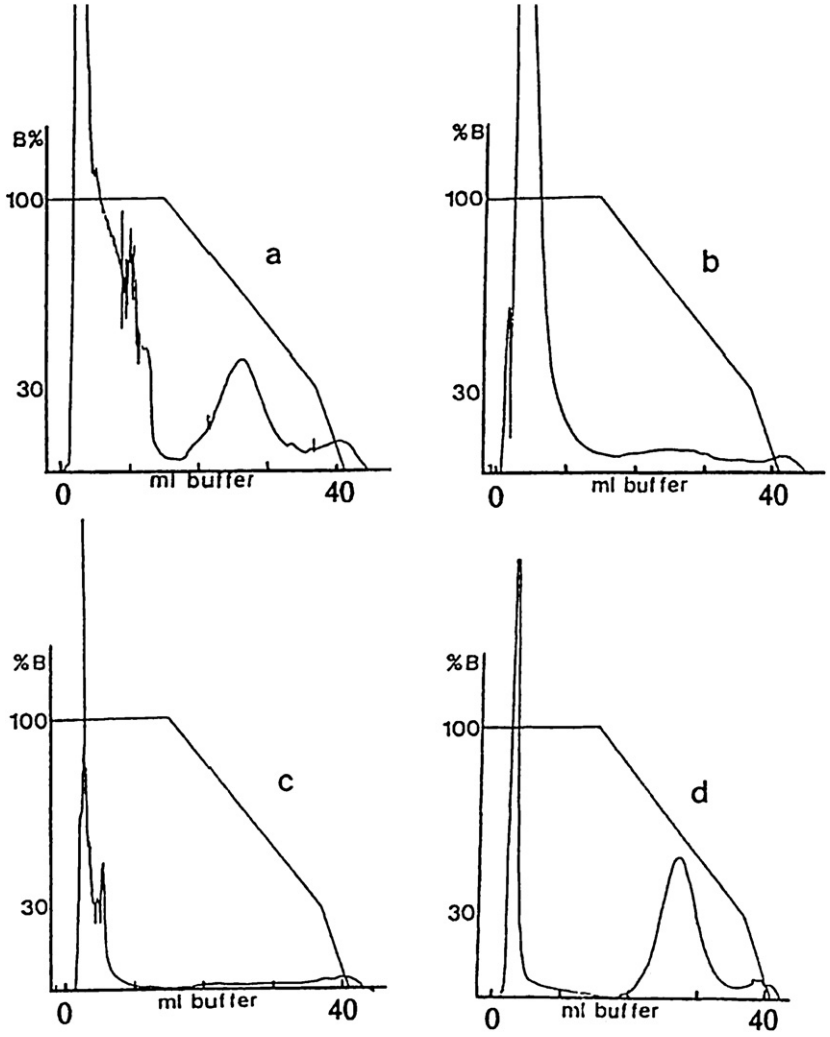

Fig. 16. Hydrophobic interaction chromatography of the top and bottom phases of extraction system I and II. (a) Extraction system I, top phase, (b) extraction system I, bottom phase, (c) extraction system II, top phase and (d) extraction system II, bottom phase [22].

Production and separation of virus and virus like particles (VLPs) has been reported. Andrews et al. [29] carried out two two-step strategies to purify yeast VLPs (virus like particles). The first strategy included a PEG 400 or 600 and $(NH_4)_2SO_4$ first stage for debris separation and a PEG 4000 or 8000 and $(NH_4)_2SO_4$ with added NaCl or phosphate for VLP purification from the proteins. The second strategy included VLP recovery in the interphase and total purification from the debris into the top PEG phase in the second stage. Benavides et al. [30], reported the use of PEG-phosphate ATPS for the recovery and partial purification of double layered Rotavirus-Like Particles (dlRLP) produced using a *Trichoplusia ni* ovary – baculovirus expression system using ATPS PEG-potassium phosphate. Liu et al. [31], studied the partition behaviour of several proteins as well as bacteriophages (such as φX174, P22, and T4) on micellar ATPS using n-decyl tetraethylene oxide ($C_{10}E_4$) as surfactant.

Table 3
Partitioning and Separation of tPA (tissue plasminogen activator) [27].

•Separation of tPA (tissue plasminogen activator), from contaminant cell culture components (CHO cell culture) in PEG/phosphate and PEG/Dextran systems
•tPA, which is a very hydrophobic protein, gave extremely high values of the partition coefficient (100–1000)
•Best separation was obtained using a PEG 1450/phosphate system pH 3 without NaCl or pH 5 with 0.5 M NaCl
•Recovery 80–100% with a purification factor of 7–12 fold (max. 19)
•Final purity 90%

7. Conclusions

Aqueous two-phase systems can be effectively used for the separation and purification of proteins.

Phase separation for ATPS formed by PEG and salts has been studied. Profiles of dispersion heights for small and larger scale systems can be represented as a fraction of the initial height and are independent of the dimensions of the separator. This is important for the design of large scale aqueous two-phase separations. Phase separations times are dependent on which of the phases is continuous. It has also been found that the phase inversion point in some systems corresponds to a fixed salt concentration (e.g. phosphate).

A continuous settler has been investigated with three different inlet geometries. Phase separation was much faster when the bottom phase is continuous. The presence of a cell extract (e.g. *B. subtilis* makes the operation much slower. The behaviour of batch and continuous systems in the presence and absence of the cell extract with continuous bottom phase shows that the settling velocity was lower in the continuous systems.

The kinetics of phase separation has been investigated as a function of the physical properties of the system. The settling rate is a

crucial parameter for equipment design and it has been investigated as a function of viscosity and density of the phases as well as the interfacial tension between them. Correlations that describe the rate of phase separation have been studied. Density and viscosity play a role in the rate of phase separation and are more dominant in the continuous top phase region. Clearly working in a continuous bottom-phase region is advantageous to ensure fast separation.

A mathematical model to describe the continuous, study state operation of these systems has been investigated. Two simulations to show the effect of phase ratio on the purification have been carried out which clearly show the effectivity of using such models.

The practical application of ATPS has been demonstrated in a large number of cases including a number of industrial applications with excellent levels of purity and yield. Very important examples include the purification of α-amylase and the large scale "in situ" purification of IGF-1 carried out by Genentech. Also the purification of monoclonal antibodies from animal cell culture supernatant and probably the production scale purification of chymosin from recombinant Aspergillus supernatant is the most successful industrial application of this technology. Other applications include the separation and purification of human α-antitrypsin from transgenic sheep milk, tPA from CHO supernatant and recombinant VLPs (virus like particles) from yeast cells.

Acknowledgement

Financial support from the Millenium Scientific Initiative (Grant ICM P05-001-F) is gratefully acknowledged.

References

[1] J.A. Asenjo, B.A. Andrews, J. Chromatogr. A 1218 (2011) 8826.
[2] P.A. Albertsson, Biochem. Pharmacol. 5 (1961) 351.
[3] P.A. Albertsson, Partition of Cell Particles and Macromolecules, Wiley, New York, 1986.
[4] P.A. Albertsson, G. Johansson, F. Tjerneld, in: J.A. Asenjo (Ed.), Separation Processes in Biotechnology, Marcel Dekker Inc., New York, 1990, p. 287.
[5] B.Y. Zaslavsky, Aqueous Two-Phase Partitioning: Physical Chemistry and Bioanalytical Applications, Marcel Dekker Inc., New York, 1995.
[6] H. Cabezas Jr., J. Chromatogr. B 680 (1996) 3.
[7] R. Hatti-Kaul, Mol. Biotechnol. 19 (2001) 269.
[8] T. Przybycien, N. Pujar, L. Steele, Curr. Opin. Biotechnol. 15 (2004) 469.
[9] D. low, R. O'Leary, N. Pujar, J. Chromatogr. B. 848 (2007) 48.
[10] P.A.J. Rosa, A.M. Azevedo, S. Sommerfeld, W. Bäcker, M.R. Aires-Barros, Biotechnol. Adv. 29 (2011) 559.
[11] P. Gagnon, J. Chromatogr. A. 1221 (2012) 57.
[12] M.H. Salamanca, J.C. Merchuk, B.A. Andrews, J.A. Asenjo, J. Chromatogr. B 711 (1998) 319.
[13] J.A. Asenjo, S.L. Mistry, B.A. Andrews, J.C. Merchuk, Biotechnol. Bioeng. 79 (2002) 217.
[14] A. Kaul, R.A.M. Pereira, J.A. Asenjo, J.C. Merchuk, Biotechnol. Bioeng. 48 (1995) 246.
[15] J.C. Merchuk, B.A. Andrews, J.A. Asenjo, J. Chromatogr. 711 (1998) 285.
[16] S.L. Mistry, A. Kaul, J.C. Melchuk, J.A. Asenjo, J. Chromatogr. 74 (1996) 151.
[17] A.S. Schmidt, A.M. Ventom, J.A. Asenjo, Enzyme Microb. Technol. 16 (1994) 131.
[18] J. Benavides, M. Rito-Palomares, J. Chem. Technol. Biotechnol. 83 (2008) 133.
[19] J. Benavides, M. Rito-Palomares, J.A. Asenjo, in: C. Webb (Ed.), Aqueous Two-Phase Systems in Comprehensive Biotechnology, vol. 2, Elsevier L.V., 2011, p. 697, doi:10.1016/B978-0-08-088504-9 00124-0.
[20] O. Cascone, B.A. Andrews, J.A. Asenjo, Enzyme Microb. Technol. 13 (1991) 629.
[21] R.A. Hart, P.M. Lester, D.H. Reifsnyder, J.R. Ogez, S.E. Builder, Biotechnology 12 (1994) 1113.
[22] B.A. Andrews, S. Nielsen, J.A. Asenjo, Bioseparation 6 (1996) 303.
[23] P.A.J. Rosa, A.M. Azevedo, S. Sommerfeld, M. Mutterb, M.R. Aires-Barros, W. Bäcker, J. Biotechnol. 139 (2009) 306.
[24] Y. Guan, T.H. Lilley, T.E. Treffry, C.-L. Zhou, P.B. Wilkinson, Enzyme Microb. Technol. 19 (1996) 446.
[25] D.P. Harris, A.T. Andrews, G. Wright, D.L. Pyle, J.A. Asenjo, Bioseparation 7 (1997) 31.
[26] K. Hayenga, M. Murphy, R. Arnold, J. Lorch, H. Heinsohn, 7th International Conference on Partitioning in ATPSs, New Orleans, USA, 1991.
[27] C. Hodgson, B.A. Andrews, V. Riveros-Moreno, J.A. Asenjo, 7th International Conference on Partitioning in ATPSs, New Orleans, USA, 1991.
[28] C. Hodgson, Partitioning and separation of tPA (Tissue Plasminogen Activator) in aqueous two-phase systems, Ph.D. Thesis, University of Reading, 1992.
[29] B.A. Andrews, R.-B. Huang, J.A. Asenjo, Bioseparation 5 (1995) 105.
[30] J. Benavides, J.A. Mena, M. Cisneros-Ruiz, O.T. Ramirez, L.A. Palomares, M. Rito-Palomares, J. Chromatogr. B 842 (2006) 48.
[31] C. Liu, D.T. Kamei, J.A. King, D.I.C. Wang, D. Blankschtein, J. Chromatogr. B 711 (1998) 127.